Entanglement Network of the Polypropylene/Polyamide Interface. 1. Self-Consistent Field Model

Andreas F. Terzis,[†] Doros N. Theodorou,*[,†,‡] and Alexander Stroeks[§]

Department of Chemical Engineering, University of Patras, GR 26500 Patras, Greece; Institute of Chemical Engineering and High-Temperature Chemical Processes, GR 26500 Patras, Greece; and DSM Research, P.O. Box 18, 6160 MD Geleen, The Netherlands

Received June 28, 1999; Revised Manuscript Received October 29, 1999

ABSTRACT: We present a lattice-based self-consistent mean-field theory of polymer interfaces composed of free and grafted chains and apply it to polypropylene/polyamide interfaces strengthened with graft copolymers. The theory takes into account the molecular weight distributions and stiffnesses of all chain species present in the system and the surface density of the copolymer. As our main interest is in the terminal mechanical properties of the interface, in our model we treat the PP/PA6 interface by envisioning an equivalent "solid" PA6 substrate on which the PP chains of the copolymeric compatibilizer are terminally grafted, extending into a bulk PP phase. All parameters of the model are obtained from experimentally known properties of the PP homopolymer. We investigate the influence of the molecular weight distribution and of the surface density of the grafted chains on bond order parameters, volume fraction profiles, and chain dimensions, as well as on the width of the region where surface-grafted and bulk PP chains intermingle. Results from the theory can be used as a starting point for generating an entanglement network representative of the interfacial region.

1. Introduction

Improving the fracture strength of immiscible polymer/polymer interfaces has been the objective of several recent experimental studies. It is common practice nowadays to improve compatibility at a polymer/polymer interface by adding or forming in situ with appropriate chemical reactions a diblock copolymer in which each block is miscible with one of the two homopolymers.[1]

It is highly desirable to develop theoretical and simulation models for predicting the structure and mechanical properties of such interfaces from the chemical constitution and architecture of their constituent chains. These models should be tested against existing experimental results and against future experimental studies of systems designed following the predictions of the models.

In this article we focus on the polypropylene/polyamide 6 (PP/PA6) system compatibilized with the reaction product between PP-*g*-MA (maleic anhydride-functionalized PP) and PA6. This system has been the subject of several experimental studies.[2−4] Moreover, both PP and PA6 are well studied, and several useful parameters are known.

The purpose of our study is to develop a hierarchical approach in order to properly model the fracture of the PP/PA6 interface under mechanical load. It is believed that ultimate mechanical properties of polymeric systems are directly related to entanglements (i.e., manifestations of hindered dynamical motion due to the topological uncrossability of the polymer molecules[1]). When each chain in a system of polymeric chains is constrained by point contacts (i.e., entanglements), we say that the system forms an entanglement network. Our objective is to develop a new algorithm in order to generate polymer entanglement networks representative of interfaces. The algorithm places large numbers of chains in continuous three-dimensional space. To form the network, the positions of all chain ends and all entanglement points must be known along each chain contour and in three-dimensional space. In our algorithm, these positions are chosen so as to conform to the density and conformation distributions given by a self-consistent field model of the interfacial region.

In this paper we develop the self-consistent field model for the PP/compatibilizer/PA6 interface. The experimental sample preparation, as described in refs 3 and 4, can serve as a guide to the "samples" we need to prepare in order to model the system. The experimental samples were made by clamping sheets of PA6 and PP* (PP + 5% PP-*g*-MA) together in an airtight, Teflon-lined mold under slight pressure and then heating the mold in a temperature-controlled oven between 185 and 220 °C. This temperature range is *above* the melting temperature of PP but *below* that of PA6. In this procedure the amount of PP−PA6 copolymer produced by the reaction between PP-*g*-MA and PA6 was changed by varying the temperature of the furnace and the length of time that the sample was left in the furnace. The formation of copolymer occurs at the interface by reaction between the maleic anhydride groups on the grafted copolymer chains and the NH_2 ends of the PA6, resulting in the formation of an imide. From the experimental literature it appears that most of the MA groups of PP-*g*-MA are located at the ends of the chains. Thus, the copolymer of PP and PA resulting from the reaction is expected to have essentially a diblock architecture.[5] No appreciable reaction of the maleic anhydride with amide linkages was detected. The in situ formation of the copolymer appears to be controlled by the diffusion of the PP* chains to the

[†] University of Patras.
[‡] Institute of Chemical Engineering and High-Temperature Chemical Processes.
[§] DSM Research.
* To whom correspondence should be addressed at the University of Patras. Phone +3061-997398, FAX +3061−993255; e-mail: doros@sequoia.chemeng.upatras.gr.

10.1021/ma991024x CCC: $19.00
Published on Web 01/27/2000

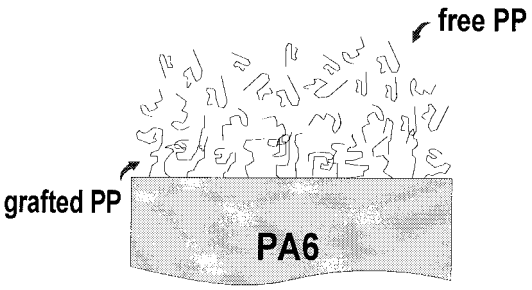

Figure 1. Schematic representation of the PP/PA6 interfacial system. The PA6 phase is represented by an equivalent "solid" substrate, on which the PP chains of the compatibilizer are terminally grafted, extending onto a bulk PP phase.

interface.[5] Under these conditions, the compatibilizer chains protruding from a PA6 crystal could be modeled as chains *grafted* onto a "solid" surface. As mentioned above, the surface density of the grafted chains is adjusted in practice by varying the annealing conditions (temperature and duration). Obviously, treating the PA6 as a solid impermeable block is a legitimate approximation as far as we do not intend to study (changes in) the structural properties of the PA6 phase. Indeed, our main focus is on the investigation of the mechanical properties of the PP/PA6 interfacial system, and there is experimental evidence (for example, TEM studies) which supports that all mechanically "important" phenomena occur within the "softer" PP region; the PA6 phase, kept together by stronger, hydrogen-bond forces, remains practically unaffected.

We have therefore considered appropriate to model the PP/PA6 interface by envisioning a crystalline PA6 matrix, treated as an equivalent "solid" substrate, on which the PP chains of the compatibilizer are terminally grafted, extending into a bulk PP phase (see Figure 1). To model realistic (i.e., consistent with the characteristics reported in the experimental studies) polymeric interfacial PP/PA6 systems, both the free and grafted PP should have a polydispersity index (PDI) different from unity (usually rather high).

A good starting point in order to describe the conformations and concentration profiles at our interface is the self-consistent mean-field lattice model (SCF), originally proposed by Scheutjens and Fleer.[6] Although bulk PP is a semicrystalline material, we represent it by means of a model (SCF) valid for amorphous polymers. This is not a bad approximation for looking at the terminal mechanical properties, given that the "soft" polyolefinic crystalline structure is quickly damaged after the early stages of deformation. A similar approximation has been invoked by Termonia and Smith to study the large-strain deformation of bulk polyolefins with an entanglement network model with very encouraging results.[7] Our intention at this stage is to formulate a first-approximation, general approach for addressing the ultimate mechanical properties of an interface between a homopolymer and a solid, strengthened by grafted chains identical in composition to the homopolymer. Experimentally, it is known that the detailed mechanism of deformation is different between crystalline and amorphous polymers. Semicrystalline morphologies can be handled within the spirit of coarse-grained entanglement network models.[8] It is our intention to build morphological details of the PP/PA6 system into the model, once our first-approximation approach proves promising. Direct Monte Carlo or molecular dynamics simulations would be an alternative way of probing the microscopic structure of our interfacial system. Steps in this direction have been taken using the lattice-based bond fluctuation model[9] as well as atomistic models.[10] Reliably simulating a system of the molecular weights of interest here over length scales relevant to fracture phenomena, however, would clearly exceed the capabilities of currently available computational resources.

2. Self-Consistent Mean-Field Lattice Model

Theoretical Formulation. The conformational statistics of an ideal chain (i.e., a chain devoid of nonlocal interactions along its contour) under the influence of an external field can be described by means of Green's functions.[11−13] As the equation followed by a Green's function is remarkably similar to the Schrödinger equation of theoretical physics, solution methods developed over the past 60 years for the Schrödinger equation can be applied to describe ideal chain statistics. It is straightforward to extend the one-chain solution to a many-chain solution only in the case where we have independent ideal chains.

To describe properly the thermodynamics of the general (from dilute to dense) many-chain system, a calculation of the free energy is required. To this end, it is convenient to inscribe (map) the many-chain system on a lattice. The continuous limit corresponds to the vanishing of the lattice parameter. Now, Green's functions of the continuous limit are replaced by segment weighting factors, which describe the probability of finding a specific chain segment at some lattice site. Although the formulation of the partition function for a dense system on a lattice and the derivation of the free energy from this partition function is not a formidable task, it is rather cumbersome or sometimes practically infeasible to derive final expressions for useful physical quantities. In most cases it is legitimate to work exclusively with the maximum term in the partition function, ignoring all other terms which are the source of the fluctuations. This approach, based on the neglect of some fluctuations in the system, is classified as a *mean-field* approximation, due to the fact that each chain is described as feeling the mean field of all surrounding chains. Usually, we describe and estimate this mean field in a *self-consistent* manner. Within an iterative procedure, the input local concentration produces a local mean field which is used in order to estimate a new conformational distribution and hence a new value for the local concentration. A self-consistent scheme is successful when the sequence of approximations for the local density converges.

A self-consistent mean-field lattice model (SCF) has been derived by Scheutjens and Fleer in order to describe the conformations and concentration profiles of a polymeric system in an interfacial region.[6,14,15] This approach has been used to describe polymer melts and polymeric solutions near a solid substrate, polymers chemically attached to the substrate, rings, branched chains, copolymers, multicomponent polymeric systems, and curved interfaces.[14] Also, the theory has been extended to incorporate conformational stiffness.[16,17]

The present work extends the Scheutjens and Fleer self-consistent field model for a system of macromolecular chains located close to a substrate. Some of the chains are terminally attached to the substrate (referred to from now on as (end) grafted chains). On the substrate it is also possible to find adsorbed (not

chemically attached) segments. We reformulate the SCF model in order to describe the most general case of free and grafted chains with various sizes (molecular weights). To develop a theoretical framework capable of describing realistic situations, the conformational stiffness is included.

A three-dimensional (xyz) lattice of simple symmetry (cubic or hexagonal) is assumed. The substrate (PA6 crystal surface) is placed parallel to the xy plane; the resulting lattice layers of the polymer (planes parallel to the surface) are numbered consecutively, starting from the layer next to the surface ($z = 1$) and ending at a layer ($z = M$) where the presence of the substrate has negligible effect. Each layer is one lattice site thick and contains L lattice sites. Each lattice site has Z neighboring sites, a fraction λ_0 of which lie in the same layer and a fraction λ_1 of which lie in each of the adjacent layers. Z, the coordination number, reflects the point symmetries characterizing the lattice ($Z = 6$ for cubic and $Z = 12$ for hexagonal; $\lambda_0 = {}^1/_2$ and $\lambda_1 = {}^1/_4$ in both lattices). To describe a constant volume system, each lattice site has to be occupied by exactly one segment. A polymer molecule is represented by a chain of r^i connected segments, numbered $s = 1, 2, ..., r^i$. The index i is adopted to denote the type of the molecule (f for free chains and g for grafted chains). No index is introduced for the segment type, as in our study both chain types (free and grafted) are of the same chemical nature (PP). An additional index j is used in order to account for the polydispersity. Thus, free (grafted) chains appear with several sizes, r_j^f (r_j^g), where j varies from a minimum (usually 1) to a maximum value. Moreover, from two consecutive segments we define the bond (b). In a cubic lattice the z-projection of a bond, reduced by the lattice constant, has three values. For two consecutive segments lying in layers z and $z + 1$, b is $+1$. For two consecutive segments lying in layers z and $z - 1$, b is -1. The value of b is 0 if both consecutive segments are lying in layer z. In other words, b (of segment s) $\equiv b_s = z_s - z_{s-1}$.

Each chain can assume a large number of possible conformations in the lattice. Each conformation (c) is defined by specifying the layer numbers in which each of the successive chain segments s finds itself (i.e., $c \equiv \{(s = 1, z = z_1), (s = 2, z = z_2), ..., (s = r_j^i, z = z_{r_j^i})\}$). The number of chains (i,j) in conformation c is indicated as $n^c_{(i,j)}$. The chains are distributed over the various possible configurations (sets of conformations $\{n^c_{(i,j)}\}$) in the lattice with statistical weights depending on the energy and entropy of each configuration. The proper description of the system will be given in the context of statistical physics by means of the grand canonical partition function. The partition function is a sum of terms, each related to a specific configuration of the chains that fills the lattice. The nonbonded chain interactions are approximated using the Bragg−Williams mean-field approximation, and the intrachain interactions are approximated using bending energies. The counting of the number of ways of arranging chains over available sites is readily performed in a lattice model. Equilibrium is the state at which the chains are distributed over the various possible conformations in the lattice such that the free energy (derived from the partition function) is at its minimum. We make the assumption of replacing the sum of several terms in the partition function by its maximum term (i.e., zero fluctuations of the density in the (x,y) directions). To obtain an expression for the number of molecules $n^c_{(i,j)}$ of chain type i of size r_j^i in conformation c, we minimize the natural logarithm of the maximum term of the partition function with respect to $n^c_{(i,j)}$, subject to the full occupancy constraint applied layerwise. It has been shown[6] that we can describe the system in a mean-field self-consistent approximation in terms of a segment potential $u(z)$ depending only on the chemical nature of the segment, or, equivalently, in terms of a segment weighting factor ($G(z) = e^{-u(z)/kT}$). The weight $G(z)$ is proportional to the probability of finding a segment in layer z of the interfacial system, relative to finding it in the bulk. Values of $G(z)$, for given layer z, very close to unity indicate that the effect of the substrate at layer z is negligible.

The $G(z,s)$, which is defined as the statistical weight for finding an end of an s-segment long chain in layer z, follows a *recursion relation*. This relation expresses the fact that, in order for the end segment of an ($s + 1$)-segment long chain to lie in layer z, its penultimate segment should reside in one of the adjacent layers ($z - 1$, z, or $z + 1$).

$$G(z,s|w) = G(z)\langle G(z,s-1|w)\rangle \tag{1}$$

where

$$\langle G(z,s-1|w)\rangle \equiv \lambda_1 G(z-1,s-1|w) + \lambda_0 G(z,s-1|w) + \lambda_1 G(z+1,s-1|w) \tag{2}$$

In eq 2, $w = 1$ corresponds to forward propagation (starting from $s = 1$) and $w = r$ corresponds to backward propagation (starting from $s = r$). To solve this recurrence relation with respect to the unknown G's, an *initial condition* is required. An obvious choice is the identification of the end segment distribution of a monomer, $G(z,1)$, with the segment weighting factor, $G(z)$.

It is straightforward to find from the end segment distributions the concentrations of the end segments. Concentrations of nonterminal segments follow by considering the probability that the segment with ranking number s within a chain of r segments finds itself in layer z as a joint probability that two walks, $s - 1$ steps and $r - s$ steps long, respectively, both end in layer z. The volume fraction $\varphi(z)$ is given by the *composition law*, which we write

$$\phi(z) = CG(z)^{-1}\sum_{s=1}^{r} G(z,s|1)\, G(z,s|r) \tag{3}$$

The constant $C \equiv n/[LG(r|1)]$, n being the number of chains with chain size r, and $G(r|1) \equiv \sum_z G(z,r|1)$ are introduced to ensure normalization. The factor $G(z)^{-1}$ is a correction for double counting, since the joining segment s is included in both walks.

This simple SCF scheme has been extended in order to treat more complex systems. One modification of the system architecture that greatly affects the conformational properties of the chains is the case of terminally grafted chains.[18,19] In addition, as most polymers are polydisperse, an extension of the SCF adsorption theory is needed in order to account for an arbitrary polymer molecular weight distribution.[20] We present here a modification of the plain SCF theory (eqs 1−3), in which both features (polydispersity and end-grafted chains) are considered simultaneously. Additionally, we properly account for conformational stiffness.[16]

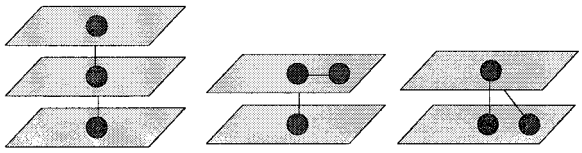

Figure 2. Three possible conformations of a trimer confined in a simple cubic lattice. In our model, the V (back-folding) conformation is prohibited.

Our first step is to introduce chain stiffness. In this model, stiffness is introduced by assigning different bending energies to different bending angles formed by triplets of segments (or pairs of bonds, see Figure 2). For a cubic lattice only 0° (back-folding or V conformer), 90° (L conformer), and 180° (straight or I conformer) bending angles are possible. The bending energies can be determined from the characteristic ratios.[16,17] To each bending energy (ϵ) we associate the corresponding Boltzmann factor $\tau = \exp(-\epsilon/kT)$. While the freely jointed chain formulation envisions the propagation of chain conformation in space as a first-order Markov process, consideration of conformational stiffness requires higher-order correlations among adjacent segments. In our formulation, initially introduced in ref 16, a second-order Markov process is considered, wherein we require the specification of two segment positions ($s - 1$ and s) by introducing a more specific end segment statistical weight $G^{b_s}(z,s|1)$. This is the statistical weight describing the case where segment s is in layer z, segment $(s - 1)$ lies in layer $(z - b_s)$, and the positions of all the other segments of that chain are summed over all possibilities. From now on, when we refer to $G(z,s|1)$ without bond index, we mean $G(z,s|1) \equiv \sum_{b_s} G^{b_s}(z,s|1)$.

The generalization of eq 1 to include chain stiffness is straightforward:

$$G^{b_s}(z,s|1) = G(z)\langle\langle G^{b_{s-1}}(z-b_s,s-1|1)\rangle\rangle \qquad (4)$$

where

$$\langle\langle G^{b_{s-1}}(z-b_s,s-1|1)\rangle\rangle \equiv \lambda_{|b_s|}\sum_{b_{s-1}} \tau_{b_{s-1}b_s} G^{b_{s-1}}(z-b_s,s-1|1) \qquad (5)$$

The bending energy contribution of each possible combination of a pair of successive bonds (b_{s-1}, b_s) is properly weighted through the factor $\tau_{b_{s-1}b_s}$. This recursion relation describes forward propagation (from segment 1 to segment s). Backward propagation (from segment r to segment s) is described by an analogous relation:

$$G^{b_{s+1}}(z,s|r) = G(z)\langle\langle G^{b_{s+2}}(z+b_{s+1},s+1|r)\rangle\rangle \qquad (6)$$

where

$$\langle\langle G^{b_{s+2}}(z+b_{s+1},s+1|r)\rangle\rangle \equiv \lambda_{|b_{s+1}|}\sum_{b_{s+2}} \tau_{b_{s+1}b_{s+2}} G^{b_{s+2}}(z+b_{s+1},s+1|r) \qquad (7)$$

The initial values can easily be guessed as $G^{b_1}(z,1|1) = G(z,1)/3$ for the forward propagation and $G^{b_{r+1}}(z,r|r) = G(z,r)/3$ for the backward propagation.

To be able to apply recursion relation 4 throughout the system, we need to define bond b_1 $(= z_{s=1} - z_{s=0})$. In that case, a "ghost" segment $s = 0$ is introduced. It is quite legitimate to assume that the three possible conformations (I, L, and V) in which the "ghost" segment is involved carry the same bending energy; hence, the respective Boltzmann factors are equal ($\tau_I = \tau_L = \tau_V = {}^1/_3$). A simple test of the validity of the latter assumption is that it leads to the correct relation for the dimer structure: $G^b(z,2|1) = \lambda_{|b|}G(z - b)G(z)$. Similarly, a "ghost" segment is added at the other end of the chain in order to define bond b_{r+1} and thus extend the applicability of the backward recursion relation up to the segment just before the last segment.

The volume fractions for a specific chain type may be found using the composition law, in which the summation has been extended to include bonds.

$$\phi(z) = CG(z)^{-1}\sum_{s=1}^{r}\sum_{b_s}\sum_{b_{s+1}} G^{b_s}(z,s|1)\tau_{b_s b_{s+1}} G^{b_{s+1}}(z,s|r) \qquad (8)$$

Expression 3 is a special case of expression 8 for equal bending energies of all possible trimer conformations (all τ equal).

Generalization to the case of polymers with an arbitrary molecular weight distribution is straightforward if the polydisperse system is considered as a "mixture" in which each "component" is a collection of chains of the same size. Following the SCF methodology, we develop a generalization of expression 8 for the case of a "mixture":

$$\phi(z) = G(z)^{-1}\sum_{k=1}^{r^{\max}}\sum_{s=1}^{k}\sum_{b_s}\sum_{b_{s+1}} C_k G^{b_s}(z,s|1)\tau_{b_s b_{s+1}} G^{b_{s+1}}(z,s|k) \qquad (9)$$

where the coefficients are $C_k \equiv n_k/[LG(k|1)]$; n_k is the number of chains with chain size k, and r corresponds to the size of the longest chains of the polydisperse polymer.

This expression, although describing correctly the volume fraction profiles in a polydisperse polymer, is not convenient for numerical calculations, as it requires the repetition of practically the same calculation as many times as the number of different chain sizes in the system. We derive a much more efficient scheme by properly rearranging the order of the summation in expression 9.

$$\phi(z) = G(z)^{-1}\sum_{s=1}^{r^{\max}}\sum_{b_s}\sum_{b_{s+1}} \tau_{b_s b_{s+1}} G^{b_s}(z,s|1)[C_s G^{b_{s+1}}(z,s|s) + G^{b_{s+1}}(z,s|\{k \geq s+1\})] \qquad (10)$$

We have introduced the chain end distribution function $(G^{b_{s+1}}(z,s|\{k \geq s+1\}) \equiv \sum_{k\geq s+1}^{r^{\max}} C_k G^{b_{s+1}}(z,s|k))$, expressing the combined statistical weight, with appropriate normalization, for segments with lengths between 1 and k. Henceforth, a recurrence relation very similar to the one holding in the monodisperse case is derived.

$$G^{b_{s+1}}(z,s|\{k \geq s+1\}) = C_{s+1}\lambda_{|b_{s+1}|}G(z)\, G(z+b_{s+1}) + G(z)\langle\langle G^{b_{s+2}}(z+b_{s+1},s+1|\{k \geq s+2\})\rangle\rangle \qquad (11)$$

where our initial condition is a straightforward gener-

alization of the monodisperse case,

$$G^{b_r}(z,r-1|\{k \geq r\}) \equiv \sum_{k \geq r} C_k G^{b_r}(z,r-1|k) = C_r G^{b_r}(z,r-1|r) \quad (12)$$

This simple SCF scheme can be extended in order to treat more complex system architectures.

One modification of the system architecture that greatly affects the conformational properties of the chains is the case of terminally grafted chains.[18,19]

In this case the chains adopt only conformations having one of their ends attached to the surface (first segment must be in first layer): $G_g^{b_1}(z,1|1) = G(z)\delta_{z,1}$.

On the contrary there are no restrictions for the free chains: $G_f^{b_1}(z,1|1) = G(z)$.

For each chain type (free/grafted) the *recursion relation* is given by eq 11, with properly modified coefficients.

The *composition law* for the free chains is given by an expression very similar to eq 10

$$\phi_f(z) = G(z)^{-1} \sum_{s=1}^{r_{\max}^f} \sum_{b_s} \sum_{b_{s+1}} \tau_{b_s b_{s+1}} G_f^{b_s}(z,s|1)[C_s^f\, G_f^{b_{s+1}}(z,s|s) + G_f^{b_{s+1}}(z,s|\{k \geq s+1\})] \quad (13)$$

For the grafted chains it is given by the following expression:

$$\phi_g(z) = G(z)^{-1} \sum_{s=1}^{r_{\max}^g} \sum_{b_s} \sum_{b_{s+1}} \tau_{b_s b_{s+1}} G_g^{b_s}(z,s|1)[C_s^f\, G_f^{b_{s+1}}(z,s|s) + G_f^{b_{s+1}}(z,s|\{k \geq s+1\})] \quad (14)$$

For a given molecular weight distribution, with number-average molecular weights $\bar{r}^f$ and $\bar{r}^g$, we can easily prove that

$$C_s^g = \sigma \frac{n_s^g}{n_{\text{total}}^g} \frac{1}{\sum_z G_f(z,s|1)} \quad \text{and}$$

$$C_s^f = \frac{M - \bar{r}^g \sigma}{\bar{r}^f} \frac{n_s^f}{n_{\text{total}}^f} \frac{1}{\sum_z G_f(z,s|1)}$$

where σ is the surface density of the end grafted chains and $n_s^{f(g)}$ is the number of free (grafted) chains with chain size s.

Mapping Real Polymers onto the Lattice. In the SCF methodology the lattice site need not be too restrictive. A detailed description might require that the lattice cell size equal the chemical monomer size. Actually, such a detailed representation may be less appropriate for modeling realistic systems, as real polymers live in continuous space and have close to tetrahedral bond angles. A description on a discrete lattice with nontetrahedral bond angles (e.g., L and I conformers only on a cubic lattice) is closer to reality on a larger (mesoscopic) scale. Obviously, the use of the lattice has the advantage of lowering the available number of configurations to a representative subset of the real configurations. Among the possible choices for the lattice segment size, the ones that have been used the most are Kuhn and Flory segments. Equating the mean-square end-to-end distance of a Kuhn chain represented by n_K Kuhn segments, each of length l_K, to the mean-square end-to-end distance of the real chain of n_b bonds, each of length l_b, with characteristic ratio, C_∞, one has

$$\langle R^2 \rangle = C_\infty n_b {l_b}^2 = n_K {l_K}^2 \quad (15)$$

Equating the maximally extended length of a Kuhn chain to the maximally extended length of a real chain, with θ_b the angle between successive chemical bonds,

$$n_K l_K = n_b l_b \sin\left(\frac{\theta_b}{2}\right) \quad (16)$$

By combining these two expressions, we find an expression for the Kuhn segment l_K,

$$l_K = l_b \frac{C_\infty}{\sin\left(\frac{\theta_b}{2}\right)} \quad (17)$$

The Flory segment, of length l_F, is usually shorter; it corresponds to the length scale at which mixing occurs. In the Flory–Huggins theory the polymer is viewed as a fully occupied lattice of site edge length l_F. In cases where the Flory parameter (χ) is used to account for attractive nonbonded interactions between segments of different chemical type, this parameter refers to a volume ${l_F}^3$. A Flory segment can be defined such that a chain will have the same maximally extended length (end-to-end distance in all-trans conformation) and volume in the Flory segment representation as are measured experimentally.[16]

Equating the volume of the Flory chain, containing r Flory segments, to the volume of a real chain:

$$r{l_F}^3 = \frac{n_m M_m}{N_A \rho} \quad (18)$$

where n_m is the degree of polymerization, M_m is the monomer molecular weight, ρ is the mass density of the polymer, and N_A is Avogadro's number.

Moreover, equating the length of the fully extended Flory chain to the maximally extended length of the real chain:

$$r l_F = n_b l_b \sin\left(\frac{\theta_b}{2}\right) \quad (19)$$

where n_b is the number of chemical bonds per chain, l_b is the bond length, and θ_b is the bond angle along the chain backbone.

By combining these equations, an expression for the length of the Flory segment is obtained,

$$l_F = \left[\frac{n_m M_m}{N_A \rho n_b l_b \sin\left(\frac{\theta_b}{2}\right)}\right]^{1/2} \quad (20)$$

The bending energies are determined from the characteristic ratios by matching the mean-square end-to-end

distance between a real chain and a chain of correlated Flory segments,

$$\langle R^2 \rangle = C_\infty n_b {l_b}^2 = C_\infty^F (r-1){l_F}^2 \quad (21)$$

in which C_∞^F is the characteristic ratio of the correlated Flory chain.

Assuming that $\tau_V = 0$ (i.e., back-folding is forbidden), the characteristic ratio of the Flory chain is related to the bending statistical weights by[16]

$$C_\infty^F = 1 + \frac{\tau_1}{2\tau_L} = 1 + \frac{1}{2} e^{(\epsilon_L - \epsilon_I)/kT} \quad (22)$$

Since the characteristic ratio depends only on the difference between the energies ($\epsilon_L - \epsilon_I$), one (in our case ϵ_I) case may be set arbitrarily to zero. From eqs 20−22, the bending energy ϵ_L can be estimated once the characteristic ratio C_∞ is known.

3. Results and Discussion

Systems Studied. We apply the SCF theory in order to investigate the interfacial properties of the PP/PA6 system. To study the PP phase by means of the SCF lattice model, we construct a lattice bounded by a flat substrate, the size of each site being equal to the polymer Flory segment.

Isotactic polypropylene is a very well studied polymer. It is known[21] that the length of the C−C bond is 1.54 Å and the angle between two consecutive C−C bonds is 112°. In ref 22 we find expressions for the density as a function of the pressure and temperature. In the results we present here we have assumed that the temperature of our system is 220 °C, which is higher than the melting point[23] and additionally is the temperature for which experimental results[3,4] on the formation of the interface are available. The value used here for the characteristic ratio (C_∞) is 5.7.[24] For this C_∞, eqs 20−22 give a bending energy $\epsilon_L = 0.402kT$ ($\tau_L = 0.669$).

For PP, the Flory segment length from eq 20 is l_F = 6.06 Å, and the number of chemical (propylene) monomers in a Flory segment is 2.37. The Kuhn statistical segment from eq 17 is l_K = 10.56 Å.

We present results for polydisperse PP with nonzero surface density of the end grafted chains. To model polydisperse samples, we need to know the molecular weight distribution. Here we present results for various molecular weight distributions. We will refer mainly to the following systems:

1. Monodisperse (PDI = 1.00) PP with number-average chain length r = 50, 200, 300, 400, 600, and 800 Flory segments (number-average molecular weight M_n = 4983, 19 930, 29 895, 39 860, 59 790, and 79 720 g/mol, respectively) for the grafted chains and r = 600 Flory segments (number-average molecular weight M_n = 59 790 g/mol) for the free chains.

2. Polydisperse PP with number-average chain length r = 200 or 400 Flory segments (M_n = 19 930 or 39 860 g/mol) for the grafted chains and r = 600 Flory segments (M_n = 59 790 g/mol) for the free chains, with various PDIs (from 1.0 for monodisperse samples to 4.8 for very polydisperse samples). To achieve the above molecular weights and polydispersities, we use (i) a uniform molecular weight distribution, (ii) the most probable (Flory) molecular weight distribution,[25] (iii) a Gaussian molecular weight distibution, (iv) the Schulz−Zimm[26] molecular weight distribution, which is a generalization of the most probable distribution, and (v) a logarithmic normal distribution[26] (i.e., a distribution where the logarithm of the weights follow a Gaussian distribution, from now on referred as lognorm), suitable for describing samples from which low-molecular-weight species have been removed.[27]

With the exception of the Gaussian and lognorm distributions, the molecular weight distributions above refer to the distribution of the numbers of chains. The Gaussian and lognorm are weight-based distributions, although in all cases the average value reported refers to the number average. The surface density (σ, in nm^{-2}) of the grafted chains is a parameter of the problem, with values ranging from 0 to 0.70 nm^{-2}.

Table 1. Free Segment Weighting Factors for a Monodisperse PP Sample with Number-Average Chain Length 400 Flory Segments for the Grafted Chains and 600 Flory Segments for the Free Chains; Each Column Corresponds to a Different Surface Density (σ) of the Grafted Chains

	$G(z)$, free segment weighting factor		
layer (z)	σ = 0.00 nm^{-2}	σ = 0.06 nm^{-2}	σ = 0.50 nm^{-2}
1	1.2526	1.2356	1.0650
2	0.9960	0.9962	0.9397
3	1.0000	0.9987	0.9309
4	1.0000	0.9988	0.9295
5	1.0000	0.9989	0.9287
6	1.0000	0.9990	0.9283
7	1.0000	0.9991	0.9281
8	1.0000	0.9992	0.9281
9	1.0000	0.9993	0.9282
10	1.0000	0.9994	0.9284
17	1.0000	0.9999	0.9312
48	1.0000	1.0000	0.9597
89	1.0000	1.0000	1.0001
...			
250	1.0000	1.0000	1.0000

Free Segment Weighting Factors and Bond Order Parameters. The simplest test we can perform in order to check the validity of our newly developed version of SCF theory is to apply this model to monodisperse PP with zero surface density of the end grafted chains. This study was performed for samples with zero bending energies and for samples with bending energies reproducing the characteristic ratios of the homopolymer (PP). For the case in which stiffness is ignored, we obtain exactly the same results as in previous studies.[14,15] It is confirmed that, for purely space filling reasons, the free segment weighting factors exhibit a damped oscillation with increasing z. When stiffness is introduced, the observed behavior depends on the bending energy. For polymers with relatively low value of the characteristic ratio (high flexibility), such as PP, the observed behavior is similar to the case in which stiffness is absent (see Tables 1 and 2). However, if a rather stiff polymer is used in the calculations (for example, polystyrene (PS) with a characteristic ratio almost twice that of PP), we observe that the oscillations of the free segment weighting factors are either shifted toward higher layers (for short chains) or altogether absent (for long chains).

For nonzero surface density of the grafted chains, we observe (Tables 1 and 2) that (a) for large surface densities, the segment statistical weights assume nonunity values for layers at appreciable distances from the interface; (b) the decay in bond order parameters with increasing z (2 orders of magnitude from first to second layer) is comparable to the one observed for the case where only free chains are present, but the order

Table 2. Bond Order Parameters of the PP Chains for a Monodisperse PP/PA6 Sample with Number-Average Chain Length 400 Flory Segments for the Grafted Chains and 600 Flory Segments for the Free Chains; Each Column Corresponds to a Different Surface Density (σ) of the Grafted Chains, and Order Parameters of the Grafted Chains Are in Parentheses

layer	$S(z)$, bond orientation order parameter		
(z)	σ = 0.00 nm^{-2}	σ = 0.06 nm^{-2}	σ = 0.50 nm^{-2}
1	−0.24664	−0.23669 (−0.24896)	−0.16067 (−0.20582)
2	+0.00327	+0.00191 (+0.00311)	+0.00925 (+0.04072)
3	−0.00003	−0.00021 (+0.00106)	+0.02305 (+0.04782)
4	0.00000	−0.00018 (+0.00108)	+0.02683 (+0.04885)
5	0.00000	−0.00018 (+0.00109)	+0.02882 (+0.04944)
6	0.00000	−0.00019 (+0.00109)	+0.02983 (+0.04975)
7	0.00000	−0.00021 (+0.00108)	+0.03031 (+0.04988)
8	0.00000	−0.00023 (+0.00109)	+0.03048 (+0.04990)
9	0.00000	−0.00025 (+0.00109)	+0.03049 (+0.04983)
10	0.00000	−0.00027 (+0.00110)	+0.03040 (+0.04970)
17	0.00000	−0.00030 (+0.00141)	+0.02890 (+0.04784)
48	0.00000	−0.00001 (+0.00628)	+0.01482 (+0.02825)
89	0.00000	0.00000 (+0.01980)	−0.00013 (+0.00970)
...			
250	0.00000	0.00000 (−)	0.00000 (−)

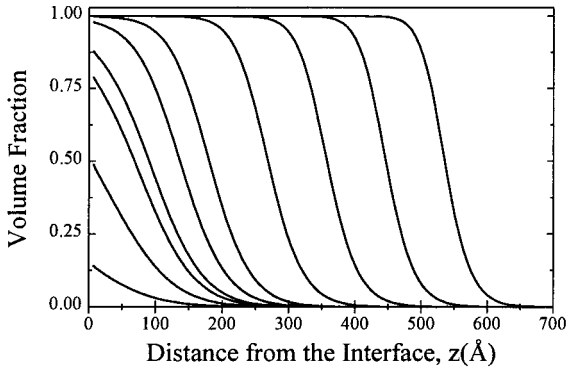

Figure 3. Volume fraction profiles of grafted chains for a monodisperse PP sample with number-average chain length 400 Flory segments for the grafted chains and 600 Flory segments for the free chains. Each curve corresponds to a different surface density (σ) of the grafted chains. The surface density increases from left to right. The values of σ used in the calculations are 0.01, 0.04, 0.08, 0.10, 0.15, 0.20, 0.30, 0.40, 0.50, and 0.60 nm^{-2}.

parameters remain nonzero up to large distances from the interface; (c) the tendency for bonds to lie flat on the surface (as perpendicular propagation against the surface is prohibited) is comparable for free and grafted chains at low surface density, but this tendency is stronger for grafted chains than for free chains as the surface density of the grafted chains is increased; and (d) for $z > 1$ (i.e., after the first layer) bonds of grafted chains are much more oriented normal to the surface (always with positive values of the bond order parameter) compared to bonds belonging to free chains.

Volume Fractions. We now study the influence of the grafting surface density on the volume fraction profiles of the grafted chains. We can always restrict our investigations to the volume fractions of the grafted chains, as the volume fractions of the free chains are simply complementary ($\varphi_f(z) = 1 - \varphi_g(z)$). Starting with the monodisperse case of chain length 600 Flory segments for the free chains and 400 Flory segments for the grafted chains, we observe (see Figure 3) a "reflected random walk" region at low surface grafting density and a "brush" region at high surface grafting density.[14] The first two surface densities ($\sigma = 0.01$ nm^{-2} and $\sigma = 0.04$ nm^{-2}) correspond to a "reflected random walk" structure

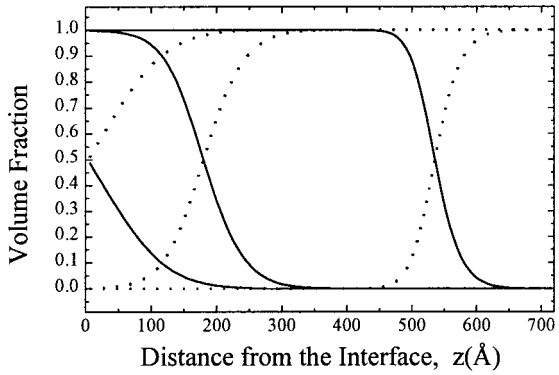

Figure 4. Volume fraction profiles of free (dotted lines) and grafted (solid lines) chains for a monodisperse PP sample with number-average chain length 400 Flory segments for the grafted chains and 600 Flory segments for the free chains. Each pair of curves corresponds to a different surface density (σ) of the grafted chains. The values of σ used are 0.04, 0.20, and 0.60 nm^{-2} (from left to right).

of the grafted chains. In these cases the dimension of a grafted chain normal to the surface is on the order of twice the radius of gyration. For the densely grafted samples ($\sigma > 0.20$ nm^{-2}), on the other hand, the first layers (closest to the interface) are occupied exclusively by grafted chains. The progressive expulsion of the free chains from the surface region when the grafting density increases has been predicted from scaling arguments by de Gennes.[28] Moreover, it is observed that, even for the densest sample ($\sigma = 0.60$ nm^{-2}), consisting of chains as long as 400 Flory segments (∼2424 Å contour length), there are no segments belonging to grafted chains beyond 650 Å. At high surface densities the region close to the interface is fully occupied by grafted chains, which are forced by their chemical grafting to have their first segment on the interface. If we plot the volume fractions of both free and grafted chains simultaneously, we have a picture of the region over which both grafted and free chains are present in appreciable amounts. These plots are depicted in Figure 4 for three representative surface densities of the grafted chains (low, intermediate, and high). The broadest regions of overlap are seen for the low (0.04 nm^{-2}) and intermediate (0.20 nm^{-2}) surface densities. For the lowest surface density (0.04 nm^{-2}), a considerable number of free (adsorbed) chains occupy sites on the interface.

Our systematic studies have shown that in order to observe a "*mushroom*" region with maximum of the volume fraction profiles of grafted chains at some distance from the interface, the free chains should be short (e.g., for grafted chains of size 400 Flory segments, the free chains should be shorter than eight Flory segments). In this case, long grafted chains are much less adsorbed by the surface than the short free chains (see Table 4.2.2 in ref 14). The reason for this behavior should be sought in the difference in space-filling ability between short and long chains (translational entropy term in the free energy). The observed behavior is in accordance with the intuitive notion that it is easier to accommodate very short chains among much longer grafted chains. In Figure 5 a "mushroom" region with maximum of the volume fraction at some distance from the interface is clearly shown for grafted chains of length 400 Flory segments and free chains of only three Flory segments (i.e., an oligomer of approximately seven chemical monomers).

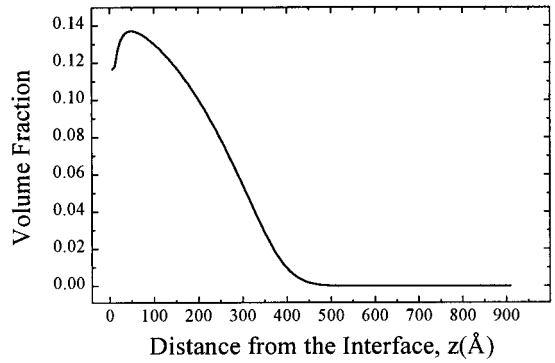

Figure 5. Volume fraction profiles of grafted chains for a monodisperse sample of length 400 Flory segments for the grafted chains and three Flory segments for the free chains. The surface density is set at 0.04 nm^{-2}.

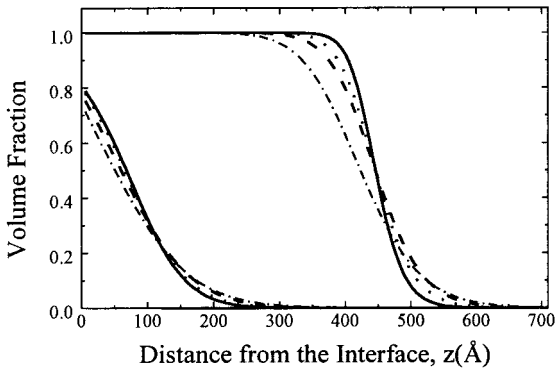

Figure 6. Volume fraction profiles of grafted chains for samples consisting of monodisperse free chains with length 600 Flory segments and polydisperse grafted chains of number-average length 400 Flory segments. The surface density is set at 0.08 nm^{-2} (left) and at 0.50 nm^{-2} (right). Each curve corresponds to a different PDI of the grafted chains. The correspondence between PDIs and line type is the following: solid line, monodisperse (PDI = 1.00); dotted line, PDI = 1.08; dashed line, PDI = 1.30; dashed/dotted line, PDI = 1.50. A uniform (flat) distribution is followed by all samples, except for the one with PDI = 1.50, which follows a Gaussian distribution.

Molecular Weight and Polydispersity Effects. We now study the influence of polydispersity on the volume fractions of the free and grafted chains. We start our study with a sample of chain size 600 Flory segments for the monodisperse free chains and of 400 Flory segments for the grafted chains. But now various polydispersity indices are assumed for the grafted chains (PDI: 1.00, 1.08, 1.30, and 1.50). For all but the last sample we assume a "uniform" molecular weight distribution. For the last sample (PDI: 1.50) we assume a Gaussian distribution. In Figure 6 we plot the volume fractions of the grafted chains for these values of the polydispersities. A surface density of $\sigma = 0.08$ nm^{-2} is assumed for the grafted chains (cluster of curves on the left-hand side of Figure 6). From these plots we conclude that polydispersity lowers the volume fraction of the grafted chains in the region close to the interface and increases the volume fractions at remote (here $z > 120$ Å) regions. This is expected, as polydispersity introduces longer chains, with increased contribution to larger distances. Similar behavior is observed in the case where we introduce polydispersity in the free chains. Exactly the same behavior is observed at a much higher surface density ($\sigma = 0.50$ nm^{-2}, cluster of curves on the right-hand side of Figure 6).

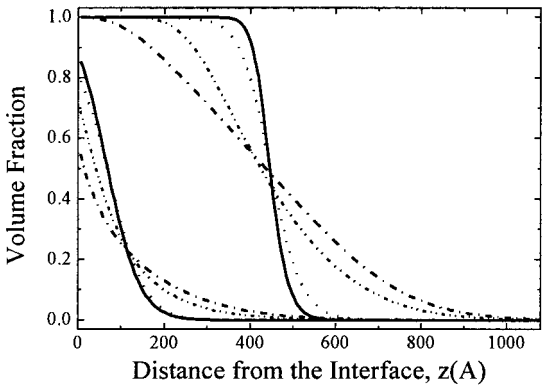

Figure 7. Volume fraction profiles of grafted chains for samples of number-average length 400 Flory segments for the grafted chains and 600 Flory segments for the free chains. Free chains are monodisperse. The surface density is set at 0.08 nm^{-2} (left) and at 0.50 nm^{-2} (right). Each curve corresponds to a different PDI of the grafted chains. The correspondence between PDIs and line type is the following: solid line, monodisperse (PDI = 1.00); dotted line, PDI = 1.30, assuming a most probable distribution; dashed/dotted line, PDI = 2.70, assuming a Schulz−Zimm distribution; dashed/double dotted line, PDI = 2.70, assuming a lognorm distribution.

To investigate further the effect of the polydispersity on the volume fraction profiles, we plot, for given surface density, the volume fraction profiles of the grafted chains for samples with different PDI and different molecular weight distributions (Figure 7). We clearly see that the Schulz−Zimm molecular weight distribution, where chains as long as 4000 Flory segments are present, exhibits the most extended volume fraction profile. To assess the influence of the type of the molecular weight distribution, we compare in Figure 7 results from samples following a Schulz−Zimm and a lognorm distribution, both showing the same PDI (∼2.7). We observe some significant difference, as the Schulz−Zimm profile is more extended and the lognorm gives significantly larger volume fraction of grafted chains in layers close to the interface. To understand this result, we should recall that in the lognorm distribution very short chains are absent, and the longest chain present is 3800 Flory segments. On the contrary, in the Schulz−Zimm even monomers are present, and the longest chain present is as long as 4000 Flory segments. We point out that lognorm is the molecular weight distribution of PP suggested by the experiments.[29]

Systematic studies of the effect of the molecular weight of the free chains have shown that the PP/PA6 system is relatively insensitive to this parameter, provided the free chains are not very short. In Figure 8 we study the effect of the molecular weight of the free chains for extreme cases and we observe a substantial difference. The effect of polydispersity is much less pronounced, as we can see from Figure 9. Actually, for a PDI of the free chains of 1.50 (Gaussian distribution, not shown in Figure 9) there is no observable difference from the monodisperse case.

Maximum Extension and Interfacial Width of Grafted Chains. To have a better understanding of the PP/PA6 interfacial system, we study the volume fraction profiles of the grafted chains (and equivalently of the free chains). One parameter that is indicative of the structure of this interfacial system is the maximum extension (z_{max}) of the grafted chains (i.e., the largest distance from the surface that a grafted chain can reach). To define z_{max}, we have to set a cutoff value for

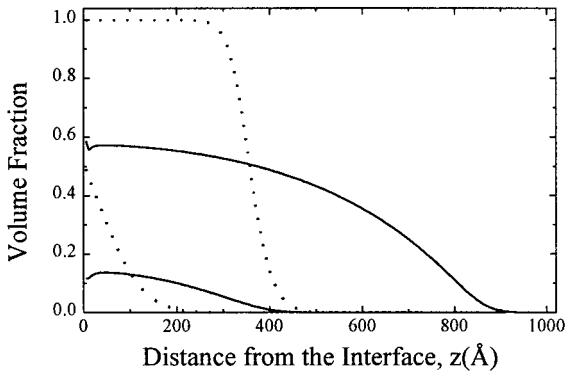

Figure 8. Volume fraction profiles of grafted chains for two monodisperse samples, both with length of the grafted chains equal to 400 Flory segments and length for the free chains three Flory segments (solid lines) and 600 Flory segments (broken lines), respectively. The two lower curves describe a system with surface density set at 0.04 nm^{-2}; for the other two curves the surface density is set at 0.40 nm^2.

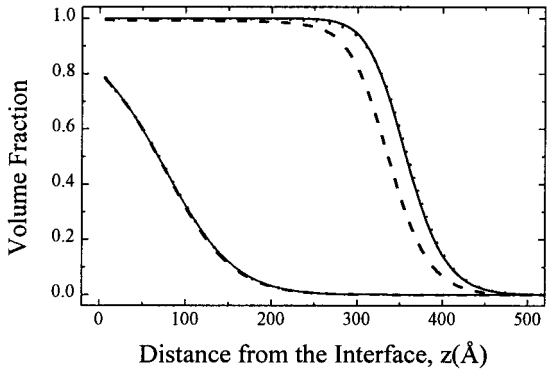

Figure 9. Volume fraction profiles of grafted chains for samples of mean length 400 Flory segments for the grafted chains and 600 Flory segments for the free chains. Grafted chains are monodisperse. The surface density is set at 0.08 nm^{-2} (left) and at 0.40 nm^{-2} (right). Each curve corresponds to a different PDI of the free chains. The correspondence between PDIs and line type is the following: solid line, monodisperse (PDI = 1.00); dashed line, PDI = 2.70, assuming a Schulz−Zimm distribution; dotted line, PDI = 4.80, assuming a lognorm distribution.

the volume fraction of the grafted chains (i.e., a low value of the volume fraction of segments of the grafted chains, below which grafted chains can be considered as absent). The dependence of z_{max} on the surface density (σ) is seen in Figure 10. A linear relationship is observed for surface densities larger than 0.10 nm^{-2}. Actually, the slope of the z_{max} vs σ curve is almost independent of the cutoff value of the volume fraction of the grafted chains used to determine z_{max} and is proportional to the average size of the grafted chains. In the $\sigma > 0.10$ nm^{-2} region a scaling law of the form $z_{max} = w' + Cl_F^3\sigma[\bar{r}^g]^\nu$ is followed, where $\nu = 1$ (global property), $\bar{r}^g$ is the number-average length of grafted chains in Flory segments, and C, the prefactor (here ~0.90), is a local property which is independent of the grafted chains. To investigate the behavior of the prefactor, we studied systems with various molecular weights of the free chains. By plotting z_{max} vs σ for systems with $r^f = 10$ Flory segments, 50 Flory segments, and 300 Flory segments, we found that the prefactor C is almost independent (see Figure 11) of the size of the free chains (0.86 for $r^f = 10$ Flory segments (not shown in Figure 11) and 50 Flory segments and 0.89 for $r^f =$ 300 Flory segments). The additive term (w') does not

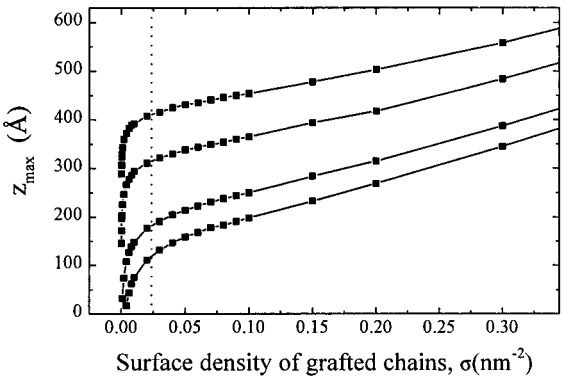

Figure 10. Plot of the maximum distance from the interface that grafted chains can reach as a function of the surface density of the grafted chains for a monodisperse PP sample with number-average chain length 400 Flory segments for the grafted chains and 600 Flory segments for the free chains. Each set of points and respective curve corresponds to a different cutoff value for the volume fraction of grafted chains used to determine z_{max}. From bottom to top the cutoff volume fractions are 0.05, 0.01, 10^{-4}, and 10^{-6}. The dashed line indicates the surface density of grafted chains at which grafted chains start touching each other. This surface density is estimated as the squared inverse of the radius of gyration of the grafted chains.

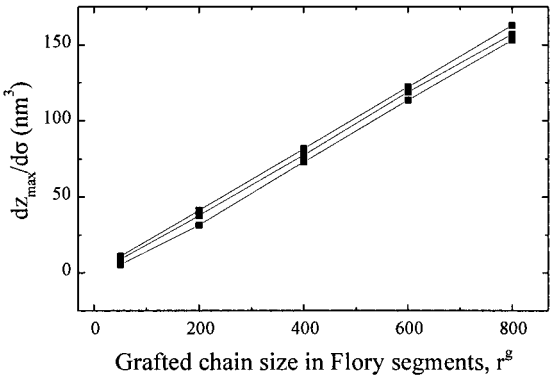

Figure 11. Plot of the slope of the (z_{max} vs σ) curve in the region of high surface grafting densities ($\sigma > 0.10$ nm^{-2}) as a function of the average size of the number-average molecular weight of the grafted chains expressed in Flory segments for various number-average molecular weights of the free chains (from bottom to top, 50, 300, and 600 Flory segments, respectively).

depend strongly on the surface density and the average molecular weight of the grafted chains. It does depend on the molecular weight distribution, as is seen from Table 3.

To test the effect of the polydispersity, we have run a variety of samples with the same number-average chain lengths (400 Flory segments for the grafted and 600 Flory segments for the free chains) but different PDIs. Results are shown in Table 3. Similar behavior is observed for all other number-average molecular weights studied.

It is known that the volume fraction profiles in the interfacial region between two immiscible homopolymers has a hyperbolic tangent functional form.[14,30] From Figure 3 we observe that, for surface densities higher than 0.20 nm^{-2}, a well-defined region of bulk grafted chains develops close to the interface (where the volume fraction of free chains is practically zero). In these cases (i.e., $\sigma > 0.20$ nm^{-2}) of high surface density, the profile of each chain type (free/grafted) can be characterized by an effective interfacial width, w, determined by a

Table 3. Maximum Distance from the Interface of Grafted Chains as a Function of the Surface Density of the Grafted Chains for Various Molecular Weight (MW) Distributions[a]

MW dist	PDI (grafted)	PDI (free)	z_{max} vs σ
monodisperse	1.00	1.00	$17.2l_F + 0.92l_F^3\,\bar{r}^g\sigma$
uniform	1.08	1.03	$17.3l_F + 0.90l_F^3\,\bar{r}^g\sigma$
uniform	1.30	1.03	$18.2l_F + 0.99l_F^3\,\bar{r}^g\sigma$
Gaussian	1.50	1.03	$21.8l_F + 0.96l_F^3\,\bar{r}^g\sigma$
uniform	1.00	1.30	$18.3l_F + 0.87l_F^3\,\bar{r}^g\sigma$
uniform	1.30	1.30	$22.6l_F + 0.93l_F^3\,\bar{r}^g\sigma$
most probable	1.30	1.30	$24.8l_F + 0.90l_F^3\,\bar{r}^g\sigma$

[a] For all samples the average size ($\bar{r}^g$) of grafted chains is 400 Flory segments and the average size of free chains ($\bar{r}^f$) is 600 Flory segments. The maximum extension (z_{max}) and the Flory segment size are measured in nm, and the surface density of the grafted chains is measured in nm^{-2}. The cutoff φ_g used to construct this table was 5%. The linear relation between z_{max} and σ is observed for $\sigma > 0.10\ nm^{-2}$.

hyperbolic tangent fit. We have

$$\phi_g(z) = \frac{e^{-2h/w}}{e^{-2h/w} + e^{2h/w}} = \frac{1}{2}\left[1 - \tanh\left(\frac{2h}{w}\right)\right] \quad (23)$$

where $h = z - z_{1/2}$.

We define $z_{1/2}$ as the layer at which the volume fraction of the grafted chains is 0.5 (i.e., equal to the volume fraction of the free chains). The interfacial width parameter, w, can be defined by means of the slope of the volume fraction of the grafted chains, since by differentiating the above equation we obtain

$$w = -\frac{1}{\left.\frac{\partial\varphi_g}{\partial h}\right]_{h=0}}$$

A maximum extension of the grafted chains can be identified by means of the length $z_{1/2} + w$. By systematic investigations we have shown that the slope of $z_{1/2}$ as a function of the surface density (σ) follows the same scaling law as the slope of the z_{max} vs σ function. For example, in the case of monodisperse free and grafted chains with $\bar{r}^f = 600$ and $\bar{r}^g = 400$, one has $z_{1/2} = 0.99l_F^3\sigma\bar{r}^g$, which can be compared to the first entry of Table 3.

Moreover, we have systematically studied the influence of the average size of the grafted chains on the maximum extension. In Figure 12 we observe that the scaling law appropriate for the more easily experimentally accessible system of low surface density of the grafted chains is in accordance with the "random coil hypothesis"; z_{max} is proportional to the square root of the average size of the grafted chains ($z_{max} \propto [\bar{r}^g]^{1/2}$, lowest curve in Figure 12). On the contrary, an almost linear relation ($z_{max} \propto \bar{r}^g$) is followed in the high surface density case (highest curve in Figure 12).

As the definition of the width by means of the hyperbolic function is useful only for interfacial systems with high surface density of grafted chains, we look for a definition of an equivalent width, which is applicable to all surface densities of the grafted chains. One choice could be the simple integral of the volume fraction of grafted chains (well defined for all possible values of surface density):

$$\int_0^\infty \phi_g\,dz$$

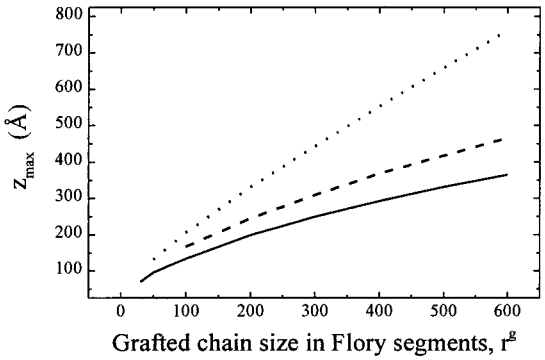

Figure 12. Plot of the maximum distance from the interface that grafted chains can reach as a function of the number-average chain length (in Flory segments) of the grafted chains, for a mondisperse PP sample with length 600 Flory segments for the free chains. Each set of points and respective curve corresponds to a different surface density of the grafted chains. From bottom to top the surface density is 0.01 nm^{-2} (solid line), 0.10 nm^{-2}(dashed line), and 0.40 nm^{-2}(dotted line). The cutoff value for the volume fraction of grafted chains used to determine z_{max} is set at 10^{-4}.

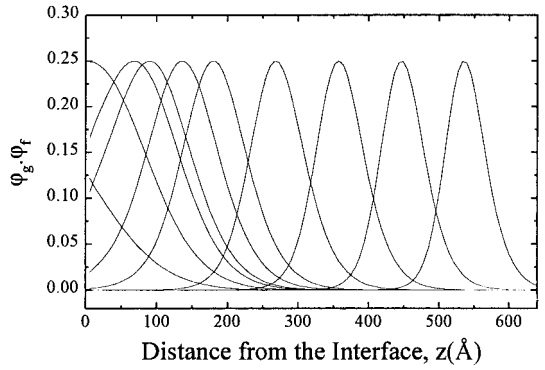

Figure 13. Profiles of the product of free and grafted chain volume fractions for a monodisperse PP sample with number-average chain length 400 Flory segments for the grafted chains and 600 Flory segments for the free chains. Each curve corresponds to a different surface density (σ) of the grafted chains. The surface density increases from left to right. The values of σ used in the calculations are 0.01, 0.04, 0.08, 0.10, 0.15, 0.20, 0.30, 0.40, 0.50, and 0.60 nm^{-2}.

However, this quantity is nothing more than the total volume per surface area occupied by the grafted chains. It follows the trivial scaling law: $\int_0^\infty \varphi_g\,dz = Cl_F^3\sigma\bar{r}^g$, where C (the prefactor) is just unity.

As our main interest is in the region where grafted and free chains coexist and can therefore interentangle, we define an interfacial width w_{int} as

$$w_{int} \equiv 4\int_0^\infty \varphi_g\varphi_f\,dz \quad (24)$$

If we apply the above definition, assuming that the volume fraction profiles follow a hyperbolic tangent profile, it can easily be shown that $w_{int} = w$ (w, the width parameter in the hyperbolic tangent function). This is an indication that our definition of the width through eq 24 is reasonable. In Figure 13 we replot Figure 1, but now the dependent variable is the product $\varphi_f\varphi_g$ and not just φ_g. Figure 13 gives an estimate of the size of regions over which free and grafted chains coexist. (The ordinate vanishes for regions where only free or grafted chains are present.) Plots of w_{int} as a function of the surface density for four systems are given in Figure 14.

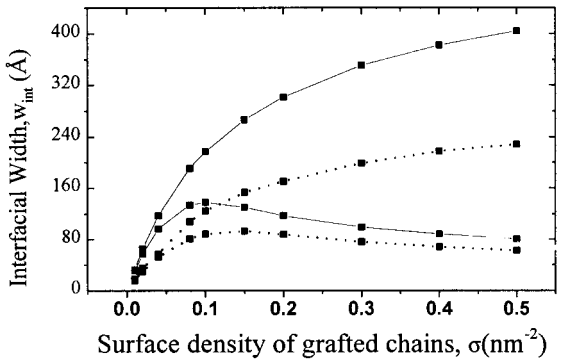

Figure 14. Plot of the effective interfacial width (w_{int}) as a function of the surface density of the grafted chains for (a) monodisperse PP sample with chain lengths 600 Flory segments for the free chains and 200 Flory segments for the grafted chains (dotted lower curve), (b) monodisperse PP sample with chain lengths 600 Flory segments for the free chains and 400 Flory segments for the grafted chains (solid lower curve), (c) polydisperse PP sample with chain lengths 600 Flory segments (PDI = 4.7) for the free chains and 200 Flory segments (PDI = 2.7) for the grafted chains (dotted upper curve), and (d) polydisperse PP sample with chain lengths 600 Flory segments (PDI = 4.7) for the free chains and 400 Flory segments (PDI = 3.3) for the grafted chains (solid upper curve). The polydisperse samples follow lognorm molecular weight distributions.

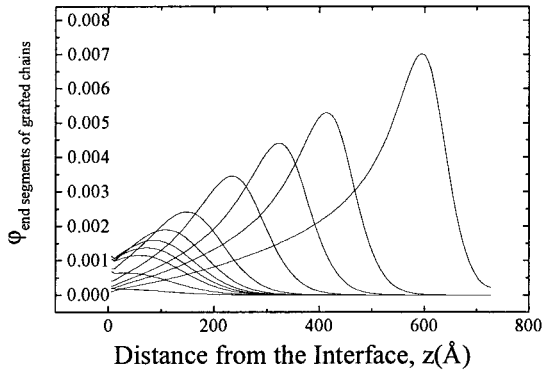

Figure 15. Profiles of the volume fractions of the free end segments of grafted chains for a monodisperse PP sample with number-average chain length 400 Flory segments for the grafted chains and 600 Flory segments for the free chains. Each curve corresponds to a different surface density (σ) of the grafted chains. The surface density increases from left to right. The values of σ used in the calculations are 0.01, 0.04, 0.08, 0.10, 0.15, 0.20, 0.30, 0.40, 0.50, 0.60, and 0.70 nm^{-2}.

Mean-Square End-to-End Distance of Grafted Chains. The extent of grafted chains can be studied by means of the mean-square z-component ($\langle R_z^2 \rangle$) of the end-to-end distance normalized by $\langle R_z^2 \rangle_0 \equiv {}^1/_3 C_\infty n_b l_b^2 \equiv {}^1/_3 n_K l_K^2$. Provided we know the volume fractions of the free ends of grafted chains, we can estimate the mean-square z-component ($\langle R_z^2 \rangle$) of the end-to-end distance by the following expression:

$$\langle R_z^2 \rangle = \frac{\int \phi_{g,ends} z^2 \, dz}{\int \phi_{g,ends} \, dz} \qquad (25)$$

In Figure 15 we show the normalized end segment volume fractions of grafted chains for a monodisperse system of grafted chains of length 400 Flory segments and of free chains of length 600 Flory segments.

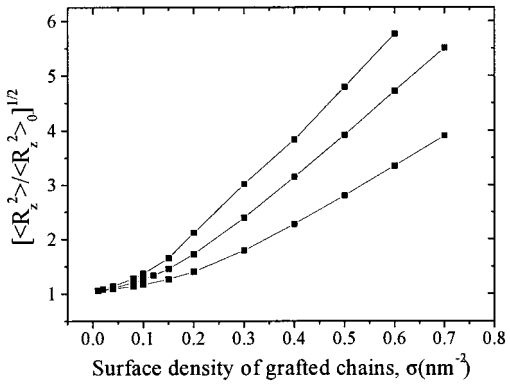

Figure 16. Plot of the normalized root-mean-square z-component ($\langle R_z^2 \rangle^{1/2}$) of the end-to-end distance of grafted chains as a function of the surface density of grafted chains, σ, for a monodisperse PP sample with chain length 600 Flory segments for the free chains and various chain lengths for the grafted chains. From bottom to top $\bar{r}^g$ = 200, 400, and 600 Flory segments.

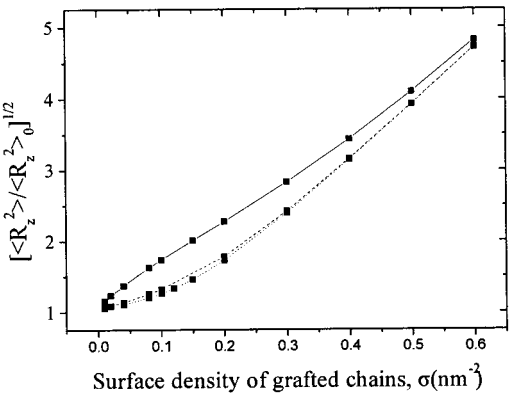

Figure 17. Plot of the normalized root-mean-square z-component ($\langle R_z^2 \rangle^{1/2}$) of the end-to-end distance of grafted chains as a function of the grafted chain surface density, σ, for a monodisperse PP sample with chain length 400 Flory segments for the grafted chains and various chain lengths for the free chains., Solid, broken, and dotted line correspond to $\bar{r}^f$ = 50, 300, and 600 Flory segments.

In Figure 16, we study the dependence of the mean-square z-component of the end-to-end distance of grafted chains on the surface density for three monodisperse systems with various grafted chain lengths. We observe a transition from random coil to brush configurations, as at low surface densities $[\langle R_z^2 \rangle / \langle R_z^2 \rangle_0]^{1/2}$ does not depend on the surface density, but at high surface densities it exhibits a linear dependence. The linear dependence on σ can be explained on simple mass balance arguments on the basis of the fact that near the surface a phase accumulates that is essentially pure grafted polymer. Thus, $\langle R_z^2 \rangle / \langle R_z^2 \rangle_0 \approx (\bar{r}^g M_0 / \rho^2 C_\infty l_b^2 N_A) \sigma^2$ where M_0 is the molecular weight per Flory segment; the slope of the linear high-σ part of the curves in Figure 16 is proportional to $(\bar{r}^g)^{1/2}$.

This behavior is not very sensitive to variations of the molecular weight of the free chains. This is confirmed in Figure 17, where we present the dependence of the mean-square z-component of the end-to-end distance on the surface density of grafted chains for three monodisperse systems with various chain lengths of the free chains. It is interesting to observe that at low grafting surface density for free chains of low molecular weight (50 Flory segments) the grafted chains do not behave

as reflected random walks but are swollen by the small-molecular-weight free chains.

4. Conclusions

The multicomponent SCF model has been extended to incorporate the effects of stiffness and to describe polydisperse interfacial systems containing free and grafted chains. This extended version of the model is applied to the investigation of the PP/PA6 interfacial system. With no parameters to fit, using values from the experimental literature, we derive structural properties (i.e., volume fraction profiles and bond order parameters). A systematic study is performed in order to understand the influence of the molecular weight distribution of grafted and free chains and the influence of the surface density of the grafted chains on the structure of the interface. From the volume fraction profiles and the bond order parameters it is concluded that the PP/PA6 interfacial system is much more sensitive to variations in the molecular weight distribution of the grafted chains than to that of the free chains. Studies of the maximum extension and of the interfacial width of realistic PP/PA6 systems (i.e., systems of high PDI of both grafted and free chains) show that, for high surface densities of the grafted chains, the grafted chains are significantly stretched. Moreover, it is observed that, to get regions next to the interface fully occupied by grafted chains, high surface densities of the grafted chains, exceeding those attained experimentally, are needed. For grafted chains in systems of very low grafted chain surface density and for free chains in systems of any surface density of the grafted chains but at remote distances from the interface, conformation follows random walk statistics. For close to monodisperse systems, the width of the region over which grafted and free chains intermingle is seen to exhibit a maximum with respect to the surface density of grafted chains; this maximum is observed at $\sigma \sim 0.1$ grafted chains/nm^{-2} for the molecular weights used in experimental work. In polydisperse systems, this maximum does not appear, but rather the interfacial width between free and grafted chains rises to an asymptotic value with increasing surface density.

Acknowledgment. Computational resources for this research were made available by the Educational and Initial Vocational Training Program on Polymer Science and Technology − 3.2a. 33H6. A.F.T. is grateful to DSM Research for financial support.

References and Notes

(1) (a) Creton, C.; Kramer, E. J.; Hui, C.-Y.; Brown, H. R. *Macromolecules* **1992**, *25*, 3075. (b) Washiyama, J.; Creton, C.; Kramer, E. J. *Macromolecules* **1992**, *25*, 4751. (c) Washiyama, J.; Kramer, E. J.; Creton, C. F.; Hui, C.-Y. *Macromolecules* **1994**, *27*, 2019.
(2) Cho, K.; Li, F. *Macromolecules* **1998**, *31*, 7495.
(3) Boucher, E.; Folkers, J. P.; Hervet, H.; Leger, L.; Creton, C. *Macromolecules* **1996**, *29*, 774.
(4) Boucher, E.; Folkers, J. P.; Creton, C.; Hervet, H.; Leger, L. *Macromolecules* **1997**, *30*, 2102.
(5) (a) Simple experiments have been performed in ref 3 (see p 777) to show that the copolymer is the dominant component for bonding a joint between PP* and PA6 and that it is formed in situ by the formation of a covalent bond between a functionalized PP chain and an NH_2 end of PA6. (b) Leger, L. Laboratoire de Physique de la Matière Condensée, Collège de France, personal communication.
(6) (a) Scheutjens, J. M. H. M.; Fleer, G. J. *J. Phys. Chem.* **1979**, *83*, 1619. (b) Scheutjens, J. M. H. M.; Fleer, G. J. *J. Phys. Chem.* **1980**, *84*, 178. (c) Scheutjens, J. M. H. M.; Fleer, G. J. *Macromolecules* **1985**, *18*, 1882.
(7) Termonia, Y.; Smith, P. *Macromolecules* **1987**, *20*, 835.
(8) Bicerano, J.; Grant, N. K.; Seitz, J. T.; Pant, K. *J. Polym. Sci., Polym. Phys.* **1997**, *35*, 2751.
(9) (a) Werner, A.; Schmid, F.; Binder, K.; Müller, M. *Macromolecules* **1996**, *29*, 8241. (b) Müller, M.; Schick, M. *J. Chem. Phys.* **1996**, *105*, 8885. Binder, K. *Monte Carlo and Molecular Dynamics Simulations in Polymer Science*; Oxford University Press: New York, 1995.
(10) Stroeks, A., unpublished results obtained with software packages from Molecular Simulations Inc., San Diego, CA.
(11) de Gennes, P. G. *Scaling Concepts in Polymer Physics*; Cornell University Press: London, 1985.
(12) Doi, M.; Edwards, S. F. *The Theory of Polymer Dynamics*; Clarendon Press: Oxford, 1986.
(13) Grosberg, Y.; Khokhlov, A. R. *Statistical Physics of Macromolecules*; AIP Series in Polymers and Complex Materials: New York, 1994.
(14) Fleer, G. J.; Cohen Stuart, M. A.; Scheutjens, J. M. H. M.; Cosgrove, T.; Vincent, *Polymers at Interfaces*; Chapman and Hall: Cambridge, 1993.
(15) Theodorou, D. N. *Macromolecules* **1988**, *21*, 1400.
(16) (a) Fischel, L. B.; Theodorou, D. N. *J. Chem. Soc., Faraday Trans.* **1995**, *91*, (b) Fischel, L. B. Molecular Modeling of Homopolymer/Copolymer/ Homopolymer Interfacial Fracture. Ph.D. Thesis, University of California, Berkeley, 1997.
(17) Wijmans, C. M.; Leermakers, F. A. M.; Fleer, G. J. *J. Chem. Phys.* **1994**, *101*, 8214.
(18) Cosgrove, T.; Heath, T.; Van Lent, B.; Leermakers, F.; Scheutjens, J. *Macromolecules* **1987**, *20*, 1692.
(19) Wijmans, C. M.; Scheutjens, J.; Zhulina, E. *Macromolecules* **1992**, *25*, 2657.
(20) Roefs, S. P. F. M.; Scheutjens, J. M. H. M.; Leermakers, F. A. M. *Macromolecules* **1994**, *27*, 4810.
(21) Mattice, W. L.; Suter, U. W. *Conformational Theory of Large Molecules*; John Wiley & Sons: New York, 1994.
(22)] (a) Zoller, P. *J. Appl. Polym. Sci.* **1979**, *23*, 1051. (b) Rodgers, P. A. *J. Appl. Polym. Sci.* **1993**, *48*, 1061.
(23) Brandrup, J.; Immergut, E. H. *Polymer Handbook*; John Wiley & Sons: New York, 1975.
(24) Boyd, R. H.; Philips. P. J. *The Science of Polymer Molecules*; Cambridge University Press: London, 1993. We use the value suggested for isotactic polypropylene in Chapter 7.6.3, "Characteristic ratios of polypropylenes".
(25) Flory, P. J. *Principles of Polymer Chemistry*; Cornell University Press: Ithaca, NY, 1981.
(26) Billmeyer, F. W., Jr. *Textbook of Polymer Science*; John Wiley & Sons: New York, 1984.
(27) Ahn, T. O.; Hong, S. C.; Kim, J. H.; Lee, D. H. *J. Appl. Polym. Sci.* **1997**, *67*, 2213.
(28) de Gennes, P. G. *Macromolecules* **1980**, *13*, 1069.
(29) Ir. Markus Bulters, DSM Research B.V., personal communication.
(30) Helfand, E.; Tagami, Y. *J. Chem. Phys.* **1971**, *56*, 3592.

MA991024X